Proceedings of the Sixth International Conference on
Railway Technology: Research, Development and Maintenance
Edited by: J. Pombo
Civil-Comp Conferences, Volume 7, Paper 10.10
Civil-Comp Press, Edinburgh, United Kingdom, 2024
ISSN: 2753-3239, doi: 10.4203/ccc.7.10.10

Simulating Solar Radiation on Railway Networks using Free and Open-Source Tools

Y. Boussad[1], A. Tomlinson[1], Y. Yang[1], S. Grant-Muller[1], C. Noakes[2], J.-A. Pattinson[1] and K.-A. Moseley[2]

[1] Institute for Transport Studies, University of Leeds, Leeds, United Kingdom
[2] School of Civil Engineering, University of Leeds, Leeds, United Kingdom

Abstract

Assessing the amount of solar radiation on trains is crucial to ensure the best performance for the air conditioning system and the best thermal comfort for the passengers. In this paper, we develop a novel methodology for simulating solar radiation on train carriages in a railway network. We use free and open-source tools and data such as Blender, OpenStreetMap, and satellite meteorological data to build a computational framework that can simulate solar irradiance on a train carriage that accounts for geographical location, time, and train orientation. First, we obtain the railway trajectory shape from OpenStreetMap and set up the simulation environment in Blender. We compute the incidence angle of solar rays on train carriages using raycasting. Then, we use solar radiation data to estimate the solar irradiance incident on the train carriage. Using this framework, we study the solar radiation on 10 different railway routes in the United Kingdom and provide a detailed spatial and temporal analysis of solar irradiance. Finally, we assess the compliance of solar radiation with the railway standards for air conditioning and thermal comfort.

Keywords: simulation, computational modelling, railway, solar radiation, open source, raycasting, GIS.

1 Introduction

The performance of the heating, ventilation and air-conditioning (HVAC) systems performance in trains can be impacted by different internal and external factors such as external temperature and solar radiation. The HVAC systems are designed to operate under certain conditions as defined in the railway standards. For instance, the European standard for air conditioning for main line rolling stock EN13129 [1] defines the maximum limit of the equivalent solar load in the summer season. In the United Kingdom (climatic zone III), the limit is 600 W/m² at an incidence angle of 30°. However, this limit does not reflect real-life conditions. The amount of solar radiation can vary depending on many factors such as weather conditions. Moreover, the angle between the solar rays and train surfaces (incidence angle) is not fixed and can change depending on the orientation of the train and the position of the sun in the sky [2].

Given the importance of HVAC system performance and its impact on the energy efficiency of modern trains [3, 4], and on providing thermal comfort for the passengers [5, 6, 1], researchers are developing models and simulations to assess the solar radiations on trains. Kim et al. [7] developed a Geographic Information System (GIS) computational algorithm for estimating the photovoltaic potential of solar trains. They computed solar irradiance on the roof of the train, accounting for the location, time, and shading from the environment and railway infrastructures by building a Digital Surface Model (DSM). Solar radiation is modelled using Earth's orbit and cycle, and the sun's location in the sky. However, this analysis is only limited to the roof irradiance and does not account for real weather conditions which can impact solar radiation intensity. Barone et al. [4] proposed a simulation tool using the TRNSYS software environment to assess the performances of the HVAC system and its energy consumption. The simulation takes into account the train's geographical position, orientation, speed, and weather conditions, and creates a weather data file for the simulation. These are then inputted to TRNSYS and simulated using a 3D model of the train.

In this work, we build a novel computational framework in a 3D environment for simulating solar radiation on a train carriage. As opposed to previous works, our methodology relies on free and open-source software and can be used to compute solar irradiance on any surface of the train carriage. Moreover, by leveraging satellite-based climate data records, it allows a realistic and accurate solar radiation estimation. We apply our methodology to 10 routes in the UK railway network, perform a spatio-temporal analysis of the solar irradiance on a train carriage, and assess compliance with the current railway standard for air conditioning and thermal comfort standards.

The choice of the 10 routes is based on: 1) a selection of routes that cover more geographical area, from the north to the south, and east to west of the UK. 2) routes that traverse the network in different directions to cover as many carriage orientations as possible. The selected routes are: London—Bristol, London—Leeds, London—Exeter, London—Norwich, London—Dover, Liverpool—Scarborough, Liverpool—Norwich, Edinburgh—Milngavie, Manchester—Bournemouth, Plymouth—Edinburgh.

2 Methods

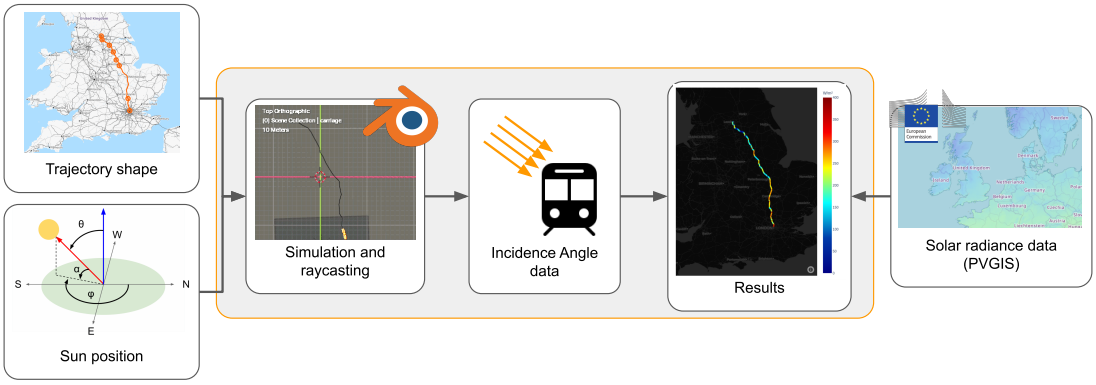

Figure 1: Computational framework for simulating solar radiation on a train carriage.

In this section, we describe our methodology for simulating solar irradiance on a train carriage. We show in Figure 1 an overview of the methodology.

2.1 Railway trajectory shape data

The first step in our methodology is getting the railway network trajectory that we want to simulate. OpenStreetMap (OSM) [8] is a free and open map data that provides various information, including but not limited to railway networks. In our case, we are interested in railway trajectories (routes), which are defined as RELATION type. We can download the route shape data from OSM as described in Appendix A. After downloading the route shape data, we convert it to a GeoJSON object using OSM2GEOJSON [9]. The final trajectory object is composed of a sequence of line segments of type SHAPELY LINESTRING.

2.2 Sun position

The next step is to position the sun properly in the 3D space. To do that, we use PVLIB [10] library to obtain the sun azimuth, elevation, and zenith angles, by providing the time and the geographical location coordinates (latitude and longitude). We do that for every line segment of the route by taking the start of each segment as location coordinates, and the time to be the first day of each month of the year, and varying the hour of the day from 4 (4 AM) to 22 (10 PM).

2.3 Raycasting and computing incidence angle

We use Blender [11] as a 3D environment for the simulation. We use the Python scripting available in Blender (bpy) to create the simulation. We start by reading the GeoJSON data to create a curve object of the railway route using the right coordinate reference system (CRS) conversion, in our case, we use EPSG:27700 [12] since we will simulate the railway network of the United Kingdom. Next, we create a cuboid object to represent the train carriage. For the sun rays, we create a grid and use the sun

position and orientation we described in Section 2.2 to position it in the 3D environment, pointing towards the train carriage. Then, we use raycasting to cast rays from each face of the grid towards the carriage.

We start the simulation by moving the train carriage along the railway trajectory. At each step, we use the starting and ending points of each segment of the trajectory to compute a vector and use it to set the orientation of the train carriage and use the centre of the segment as the carriage position. Once the carriage is well positioned, we cast rays from each face of the raycasting grid, and check for collisions with the train carriage geometry, as shown in Figure 2. For each collision, we compute the angle between the ray vector and the normal of the train carriage face hit by the ray. From this, we can obtain the *incidence angle* of the sun rays on the train carriage. We repeat this process for each segment of the trajectory.

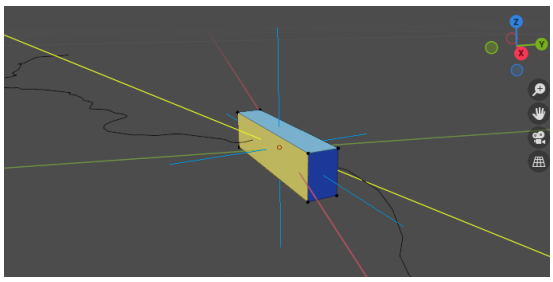

Figure 2: Raycasting solar rays (yellow line) on train carriage moving along the railway trajectory (black line). The incidence angle is computed from the angle between the solar ray and the train surface normal (blue line) hit by the ray.

From the incidence angle, we can compute the radiation intensity on the surface using Lambert's cosine law [13, 14], which states that the radiation intensity (I) is proportional to the cosine of the angle between the ray and the normal of the surface hit by the ray ($\theta_{incidence}$).

$$I \propto cos(\theta_{incidence}) \tag{1}$$

2.4 Satellite solar radiation data

After computing the incidence angle of solar rays on the train carriage as it moves along the railway trajectory, we need to combine it with solar radiation intensity values. For that, we use the Photovoltaic Geographical Information System (PVGIS) that provides solar radiation data for any given location. It uses The Surface Solar Radiation Data Set-Heliosat (SARAH), which is a satellite-derived dataset of all-sky irradiance [15, 16]. It offers a wide range of data at different granularity levels (monthly, daily, hourly). It also provides Typical Meteorological Year (TMY) data that can be downloaded using a dedicated API [17].

TMY is hourly meteorological data for the whole year for a given geographical location, selected from hourly data in a longer period (10 years or more). *"For each month in the year, the data have been selected from the year that was considered most 'typical' for that month."* [18]. We use the coordinates of the first point of each segment

in the trajectory as location coordinates when fetching TMY data. From the TMY data, we use the Direct (beam) normal irradiance (G_{bn}), and we multiply it by the cosine of the incidence angles to obtain the solar irradiance on the train carriage.

$$I = G_{bn} \cdot cos(\theta_{incidence}) \quad (W/m^2) \tag{2}$$

It's worth noting that TMY time, given in UTC format, has to be converted to the corresponding time zone, accounting for daylight saving, before the analysis.

3 Results

In this section we present the results of applying the methodology we described in Section 2 on a set of 10 railway routes in the United Kingdom. Table 1 shows a description of the different routes in terms of number of line segments, the length of the segments, and the total distance of the route.

	Number of segments	minimum (m)	mean (m)	median (m)	maximum (m)	Total distance (m)
London — Bristol	82	287	2310	1836	12406	189439
London — Leeds	140	48	2133	1473	13024	298575
Edinburgh — Milngavie	57	388	1486	1222	6576	84722
Liverpool — Scarborough	136	288	1705	1207	17941	231880
Plymouth — Edinburgh	524	203	1717	1311	18680	899718
London — Exeter	140	41	1975	1514	25341	276456
Liverpool — Norwich	232	48	1733	1042	17941	402120
Manchester — Bournemouth	255	28	1603	1341	6487	408882
London — Dover	80	36	1546	1348	5297	123702
London — Norwich	82	327	2253	1556	13224	184766

Table 1: Description of the selected railway routes. Each route is composed of line segments of different lengths (in meters).

Figure 3 shows the distribution of the direct normal radiation G_{bn} obtained from the TMY data for different seasons. The radiation is very low during winter (Dec, Jan, Feb) and fall (Sep, Oct, Nov) seasons, and higher during the spring (Mar, Apr, May) and summer (Jun, Jul, Aug) seasons as the weather conditions improve and the increase of daylight time after the winter solstice, especially in the south part of England during the summer season (London—Exeter, London—Dover, and London—Norwich).

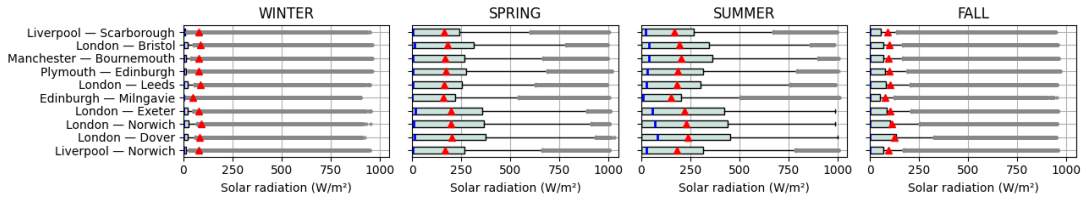

Figure 3: Distribution of the direct (beam) normal radiation (TMY data). The median and mean values are shown in blue and red, respectively.

From the incidence angles obtained from the simulations, we compute the proportion of solar radiation on the train carriage in different seasons. As defined in Equation (1),

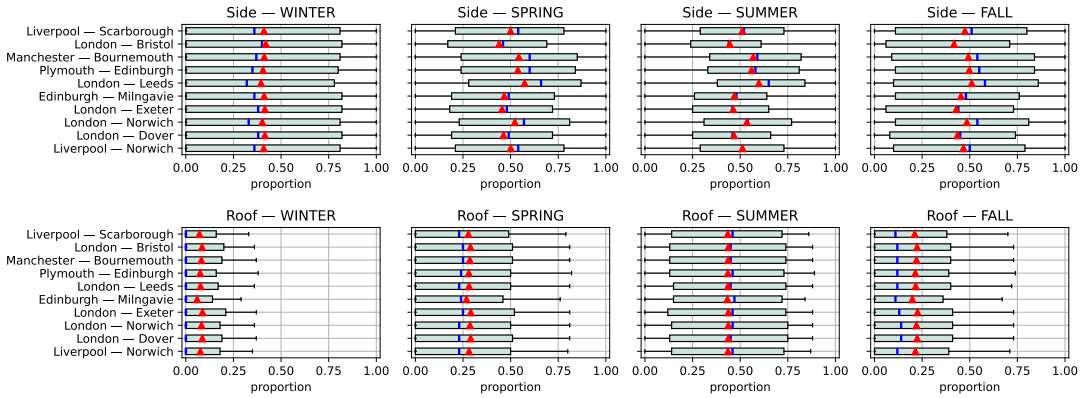

Figure 4: Distribution of irradiance proportion $(cos(\theta_{incidence}))$ on the side and roof of train carriage for different seasons. The median and mean values are shown in blue and red, respectively.

the intensity of solar radiation is proportional to the cosine of the incidence angle between the sun rays and the normal of the surface $(cos(\theta_{incidence}))$. The results are shown in Figure 4.

For the two side surfaces of the train carriage, the proportion varies a lot during the winter season, with a relatively low average of 0.4 (40%). During the spring season, the proportions have less variability, with half of the values being between 0.25 and 0.75, and averaging around 0.50. Moreover, the proportions are different across the different railway routes. Train carriage on the London—Leeds trajectory absorbs the highest proportion of solar radiation with a median value of 0.65, followed by Plymouth—Edinburgh and Manchester—Bournemouth, with the lowest exposure in the London—Bristol route. During summer, the average proportions increase slightly compared to spring, with lesser variability. During the fall season, the proportions decrease to under 0.50, and an increase in variability similar to the winter season. For the roof face of the train carriage, there are no clear differences between the railway routes in terms of proportions. In winter, the solar proportion is lowest, at about 0.08 only. This increases to 0.28 during spring, and reaches 0.44 during the summer, to decrease again during fall to 0.22 on average.

Figure 5 shows the spatial analysis of the solar irradiance proportions on the sides as well as the roof of the train carriage. The sides of the train carriage are evenly exposed to solar radiation during winter. In spring and summer, more proportion of solar radiation is absorbed in parts of the railway network that are oriented north – south and north-east – south-west, compared to east – west orientation. This effect is less prominent during the fall season. However, for the roof of the carriage, to proportions are highest during summer, and lowest during winter.

By using the TMY data, we can quantify the solar irradiance on the train carriage using Equation (2). Figure 6 shows the distribution of solar irradiance on the sides and the roof of the train carriage for different seasons. The irradiance is lowest during the winter season, with average irradiance of 50 W/m² and 10 W/m² for the sides and roof,

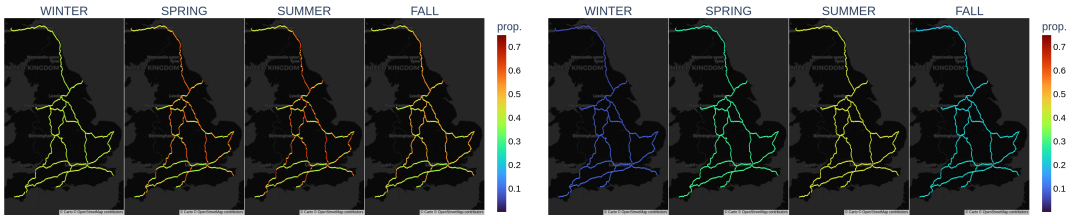

(a) Side (b) Roof

Figure 5: Average irradiance proportion $(cos(\theta_{incidence}))$ on the sides and the roof of the train carriage.

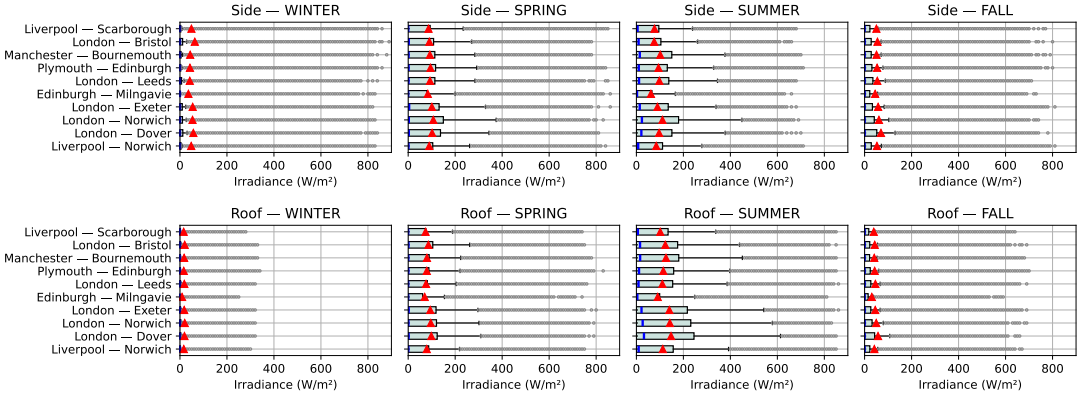

Figure 6: Distribution of solar irradiance.

respectively. It increases during spring and summer to around 100 W/m² on average and drops again to around 50 W/m² during fall. We also notice that the irradiance is higher in railway routes that are in the south part of England, and lowest in northern routes.

Figure 6 shows a lot of irradiance values as outliers (shown in grey colour). Here, we quantify the probability (frequency) of irradiance exceeding the solar load limit defined in EN13129 standard [1] of $600 \cdot cos(30°)$ W/m² and $600 \cdot sin(30°)$ W/m² during the summer season for the side and the roof, respectively. To do that, and using Equation 3, we compute the frequency of irradiance exceeding the limit for each segment in the railway route, and then we compute the weighted average for each route using the segment length (distance) as weights. The results are shown in Table 2.

$$P_{excess}^{Route} = \frac{\sum_{seg=1}^{k} (\frac{d_{seg}}{n} \cdot \sum_{i=1}^{n} [I_i^{seg} > limit])}{\sum_{seg=1}^{k} d_{seg}} \tag{3}$$

Where I_i^{seg} is the i^{th} summer solar irradiance on the train carriage along the line segment seg with length d_{seg} on the railway route $Route$.

Some railway routes (Manchester—Bournemouth, Plymouth—Edinburgh, London—Leeds, London—Norwich) are more susceptible to exceeding the radiation limit on the side of the carriage than other routes (London—Bristol, Edinburgh—Milngavie,

London—Exeter). However, the probabilities are all under 5%. For the roof exposure, the probability of exceeding the limit varies between 11% to 21% for all routes. Southern trajectories (London—Bristol, Manchester—Bournemouth, London—Exeter, London—Norwich, London—Dover) have a higher chance of exceeding the limit by more than 16% chance.

	SIDE	ROOF
London — Bristol	0.4	**16.9**
London — Leeds	**2.9**	14.8
Edinburgh — Milngavie	0.5	11.4
Liverpool — Scarborough	1.2	12.9
Plymouth — Edinburgh	**2.5**	15.1
London — Exeter	0.5	**19.7**
Liverpool — Norwich	1.4	15.5
Manchester — Bournemouth	**3.0**	**17.3**
London — Dover	1.0	**21.1**
London — Norwich	**2.5**	**19.8**

Table 2: Probability of exceeding the solar load limit (EN13129).

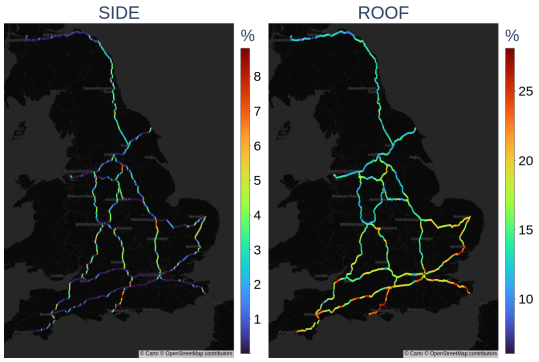

Figure 7: Probability map of exceeding the solar load limit (EN13129).

Figure 7 reveals the parts of the railway routes that are more susceptible to exceeding the radiation limit. As we discussed previously, the sides have higher chances of exceeding the limit in railway trajectories that are oriented north – south and north-east – south-west, namely near Norwich on the London—Norwich route, between Peterborough and London on the London—Leeds route, and near Bournemouth. For the roof irradiance, the southern parts of the railway routes are more susceptible to exceeding the limit. As we move northward, the probability decreases. In summary, London—Norwich, London—Dover, and Manchester—Bournemouth have the highest risk of exceeding the solar radiation limit, and Edinburgh—Milngavie has the lowest risk.

4 Conclusions and Contributions

In this work, we presented a computational framework for simulating solar irradiance on a train carriage, which accounts for the railway network shape for train orientation, time of the day and period of the year, and geographical and meteorological conditions from satellite data. We used free and open-source tools and data sources such as Blender, OpenStreetMap, and PVGIS to create our simulation framework. We have shown how it can be used to assess the exposure to solar radiation, both in time as well as in space. In addition to that, it can estimate solar irradiance on any face of the train carriage, not only the roof.

In conclusion, this work demonstrates how free and open-source tools and data can be used to build a simulation framework to study solar radiation on railway networks. This framework can be further extended to study solar exposure on passengers inside the train carriage by using a realistic 3D model instead of a simple cuboid. This will allow a more accurate modelling of thermal comfort, energy consumption and

performances of HVAC systems. A more accurate simulation can be achieved by accounting for railway infrastructure such as tunnels and shading from the environment using DSM and limiting the analysis to a specific period of the day or to the scheduled train timetable hours for each route.

Acknowledgements

This work was supported by the Engineering and Physical Sciences Research Council with grant reference IAA4081.

Appendix A Downloading railway shape data

We can download railway route shape data from OpenStreetMap (OSM). For that, we use the following URL format `https://www.openstreetmap.org/api/0.6/relation/RELATION_ID/full`, where `RELATION_ID` is the unique OSM identifier of the route.

References

[1] "European standards BS EN 13129:2016 Railway applications. Air conditioning for main line rolling stock. Comfort parameters and type tests," May 2024.

[2] H. G. Deroux M., "Investigation of sun shading effects on rail vehicles in urban areas," *Railvolution*, Jan. 2011.

[3] A. González-Gil, R. Palacin, P. Batty, and J. P. Powell, "A systems approach to reduce urban rail energy consumption," *Energy Convers. Manage.*, vol. 80, pp. 509–524, Apr. 2014.

[4] G. Barone, A. Buonomano, C. Forzano, and A. Palombo, "Enhancing trains envelope – heating, ventilation, and air conditioning systems: A new dynamic simulation approach for energy, economic, environmental impact and thermal comfort analyses," *Energy*, vol. 204, p. 117833, Aug. 2020.

[5] W. Zhou, M. Yang, X. Yu, Y. Peng, C. Fan, D. Xu, and Q. Xiao, "Enhancing thermal comfort prediction in high-speed trains through machine learning and physiological signals integration," *J. Therm. Biol.*, vol. 121, p. 103828, Apr. 2024.

[6] L. Yang, X. Li, and J. Tu, "Thermal comfort analysis of a high-speed train cabin considering the solar radiation effects," *Indoor Built Environ.*, vol. 29, no. 8, pp. 1101–1117, Sep. 2019.

[7] H. Kim, J. Ku, S.-M. Kim, and H.-D. Park, "A new GIS-based algorithm to estimate photovoltaic potential of solar train: Case study in Gyeongbu line, Korea," *Renewable Energy*, vol. 190, pp. 713–729, May 2022.

[8] "OpenStreetMap," May 2024, [Online; accessed 10. May 2024]. [Online]. Available: https://www.openstreetmap.org

[9] aspectumapp, "osm2geojson," May 2024, [Online; accessed 13. May 2024]. [Online]. Available: https://github.com/aspectumapp/osm2geojson

[10] K. S. Anderson, C. W. Hansen, W. F. Holmgren, A. R. Jensen, M. A. Mikofski, and A. Driesse, "pvlib python: 2023 project update," *Journal of Open Source Software*, vol. 8, no. 92, p. 5994, Dec. 2023.

[11] Blender Foundation, "blender.org - Home of the Blender project - Free and Open 3D Creation Software," May 2024, [Online; accessed 13. May 2024]. [Online]. Available: https://www.blender.org

[12] Klokan Technologies GmbH (https://www.klokantech.com/), "OSGB36 / British National Grid - United Kingdom Ordnance Survey - EPSG:27700," May 2024, [Online; accessed 14. May 2024]. [Online]. Available: https://epsg.io/27700

[13] J. Folkesson, H. Chang, and N. Bore, "Lambert's Cosine Law and Sidescan Sonar Modeling," in *2020 IEEE/OES Autonomous Underwater Vehicles Symposium (AUV)*. IEEE, 2020, pp. 2020–02.

[14] P. Shirley, M. Ashikhmin, and S. Marschner, *Fundamentals of Computer Graphics*. Boca Raton, FL, USA: CRC Press, Jul. 2005.

[15] "Photovoltaic Geographical Information System (PVGIS)," May 2024, [Online; accessed 14. May 2024]. [Online]. Available: https://joint-research-centre.ec.europa.eu/photovoltaic-geographical-information-system-pvgis_en

[16] "EUMETSAT - Product Navigator - Surface Solar Radiation Data Set - Heliosat (SARAH) - Edition 2," Jul. 2021, [Online; accessed 20. May 2024]. [Online]. Available: https://navigator.eumetsat.int/product/EO:EUM:CM:MULT:SARAH_V002

[17] "API non-interactive service," May 2024, [Online; accessed 14. May 2024]. [Online]. Available: https://joint-research-centre.ec.europa.eu/photovoltaic-geographical-information-system-pvgis/getting-started-pvgis/api-non-interactive-service_en

[18] "Typical Meteorological Year (TMY)," May 2024, [Online; accessed 14. May 2024]. [Online]. Available: https://e3p.jrc.ec.europa.eu/articles/typical-meteorological-year-tmy